Redox Modulation of Field-Induced Tetrathiafulvalene-Based Single-Molecule Magnets of Dysprosium

Siham Tiaouinine,[1,2] *Jessica Flores Gonzalez*[1], *Vincent Montigaud*[1], *Carlo Andrea Mattei*[1], *Vincent Dorcet,*[1] *Lakhmici Kaboub*[1], *Vladimir Cherkasov,*[3] *Olivier Cador*[1], *Boris le Guennic*[1], *Lahcène Ouahab,*[1] *Viacheslav Kuropatov,*[3]* *Fabrice Pointillart*[1]*

[1] Univ Rennes, CNRS, ISCR (Institut des Sciences Chimiques de Rennes) - UMR 6226, F-35000 Rennes, France

[2] Laboratory of Organic Materials and Heterochemistry, University of Tebessa, Algeria

[3] G. A. Razuvaev Institute of Organometallic Chemistry of Russian Academy of Sciences, 603950, GSP-445, Tropinina str., 49, Nizhny Novgorod, Russia

* Correspondence: fabrice.pointillart@univ-rennes1.fr,

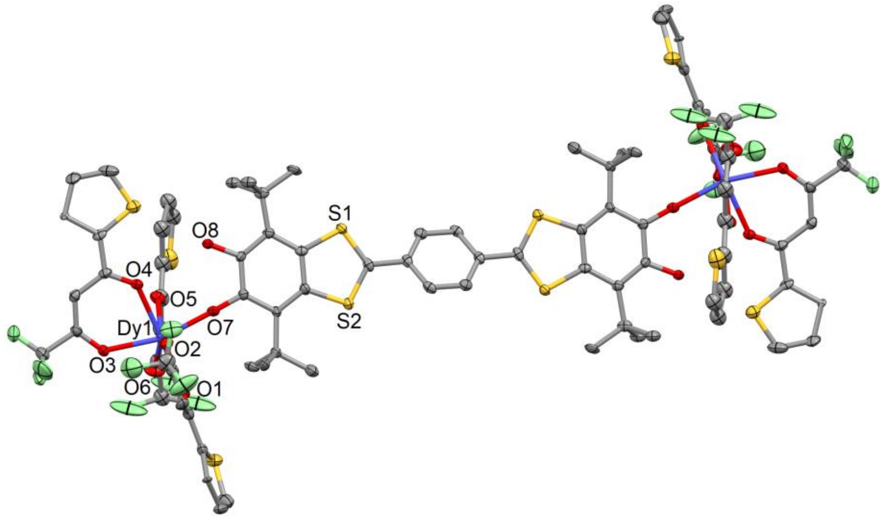

Figure S1. ORTEP view of **Dy-H₂SQ**. Thermal ellipsoids are drawn at 30% probability. Hydrogen atoms are omitted for clarity.

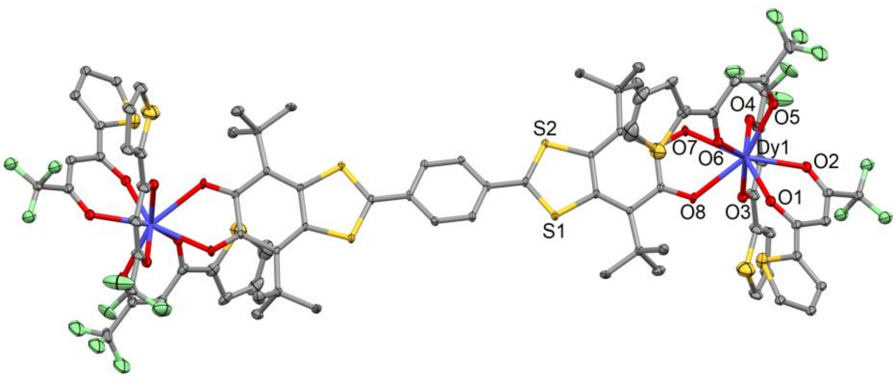

Figure S2. ORTEP view of **Dy-Q**. Thermal ellipsoids are drawn at 30% probability. Hydrogen atoms and solvent molecules of crystallization are omitted for clarity.

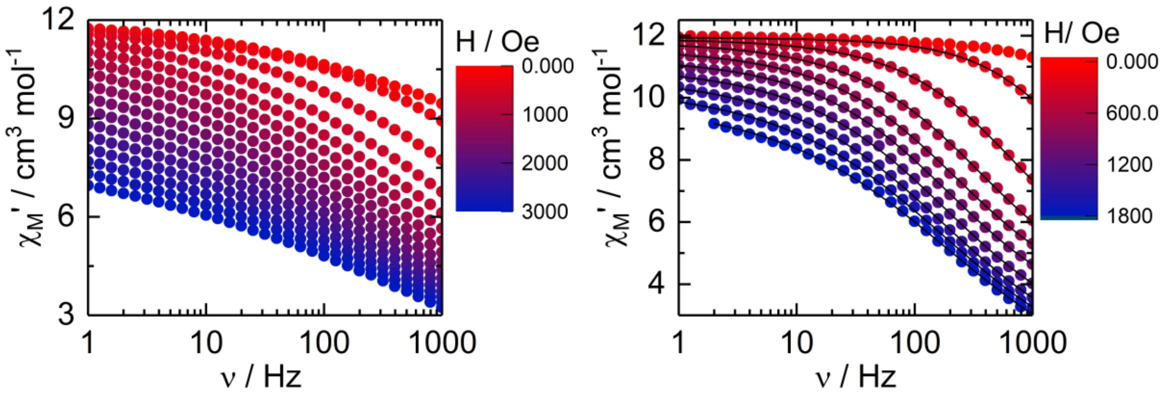

Figure S3. (left) Frequency dependence of χ_M’ between 0 and 3000 Oe for **Dy-H2SQ** at 2K, (b) Frequency dependence of χ_M’ between 0 and 1600 Oe for **Dy-Q** at 2 K with the best fitted curves.

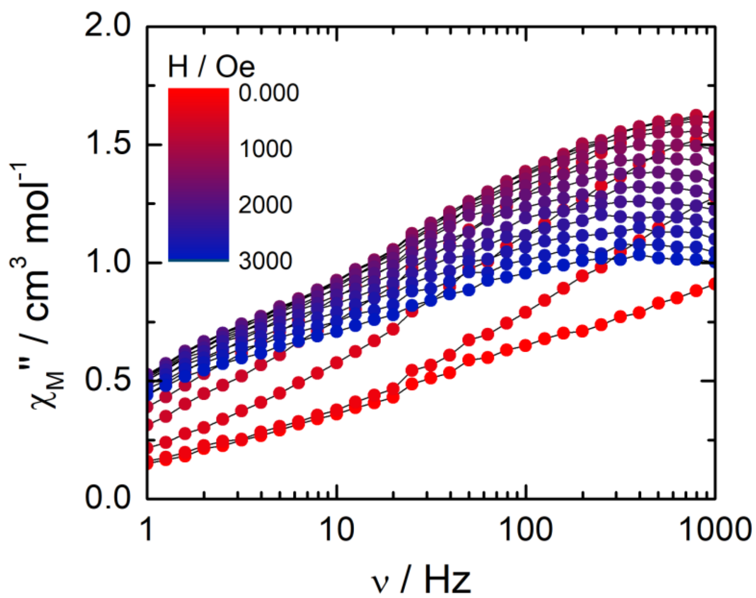

Figure S4. Frequency dependence of χ_M” between 0 and 3000 Oe for **Dy-H2SQ** at 2K.

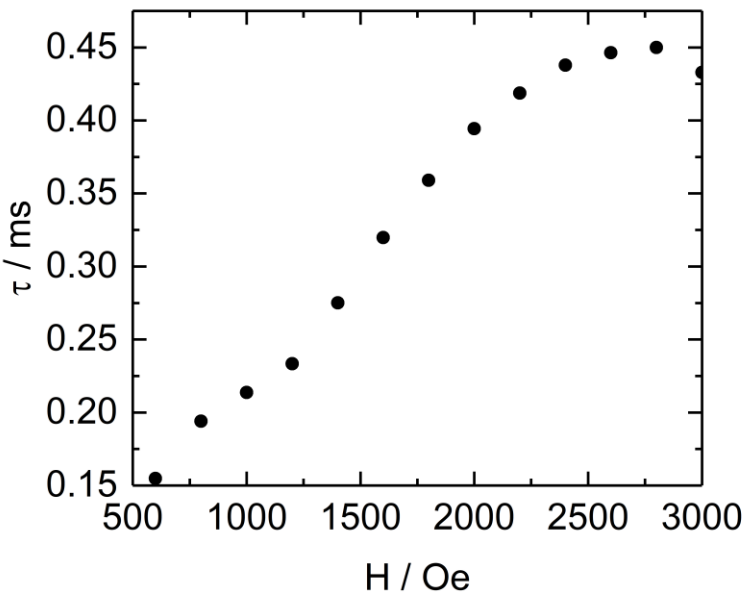

Figure S5. Representation of the field-dependence of the relaxation time of the magnetization for **Dy-H_2SQ** at 2 K.

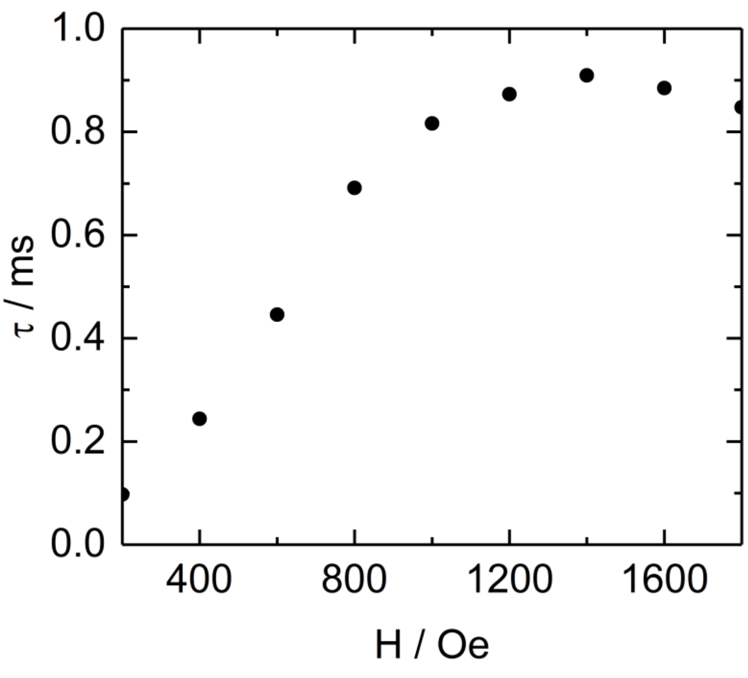

Figure S6. Representation of the field-dependence of the relaxation time of the magnetization for **Dy-Q** at 2 K.

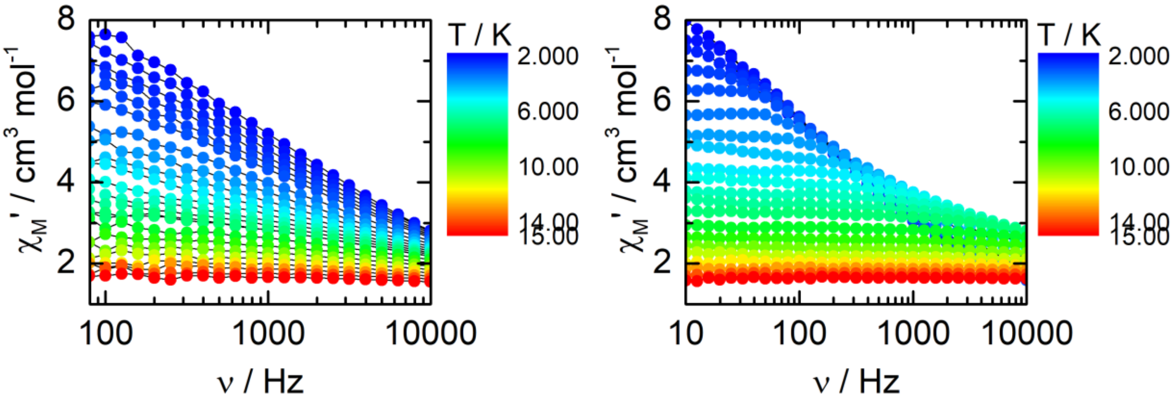

Figure S7. Frequency dependence of χ_M' between 2 and 15 K at 1200 Oe for **Dy-H$_2$SQ** (left) and **Dy-Q** (right).

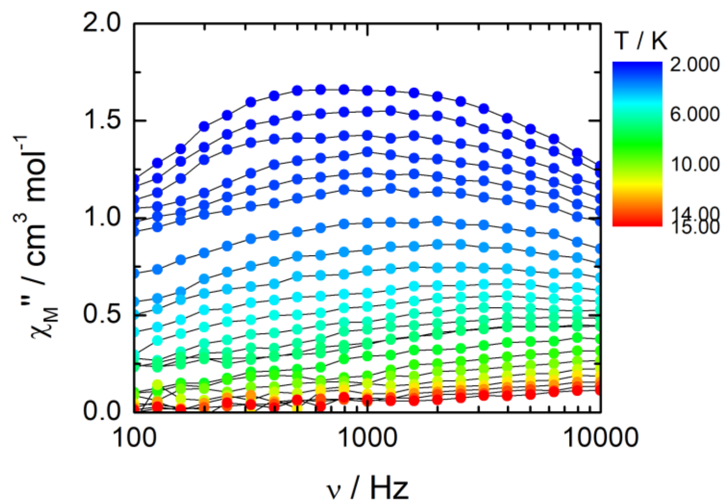

Figure S8. Frequency dependence of χ_M" between 2 and 15 K for **Dy-H$_2$SQ** at 1200 Oe.

Extended Debye model.

$$\chi_M' = \chi_S + (\chi_T - \chi_S)\frac{1+(\omega\tau)^{1-\alpha}\sin\left(\alpha\frac{\pi}{2}\right)}{1+2(\omega\tau)^{1-\alpha}\sin\left(\alpha\frac{\pi}{2}\right)+(\omega\tau)^{2-2\alpha}}$$

$$\chi_M'' = (\chi_T - \chi_S)\frac{(\omega\tau)^{1-\alpha}\cos\left(\alpha\frac{\pi}{2}\right)}{1+2(\omega\tau)^{1-\alpha}\sin\left(\alpha\frac{\pi}{2}\right)+(\omega\tau)^{2-2\alpha}}$$

With χ_T the isothermal susceptibility, χ_S the adiabatic susceptibility, τ the relaxation time and α an empiric parameter which describe the distribution of the relaxation time. For SMM with only one relaxation time, α is close to zero. The extended Debye model was applied to fit simultaneously the experimental variations of χ_M' and χ_M'' with the frequency ν of the oscillating field ($\omega = 2\pi\nu$). Typically, only the temperatures for which a maximum on the χ'' vs. *f* curves, have been considered. The best fitted parameters τ, α, χ_T, χ_S are listed in Table S2 with the coefficient of determination R^2.

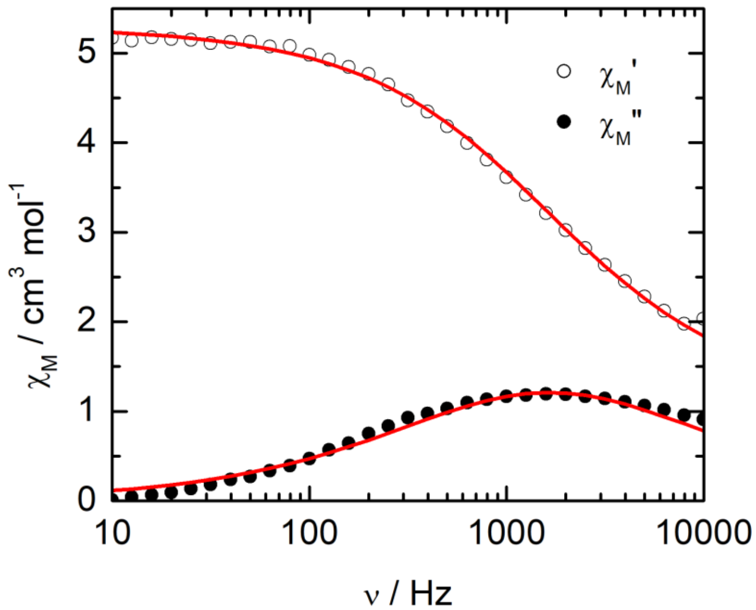

Figure S9. Frequency dependence of the in-phase (χ_M') and out-of-phase (χ_M'') components of the ac susceptibility measured on powder at 4 K and 1200 Oe with the best fitted curves (red lines) for **Dy-Q**.

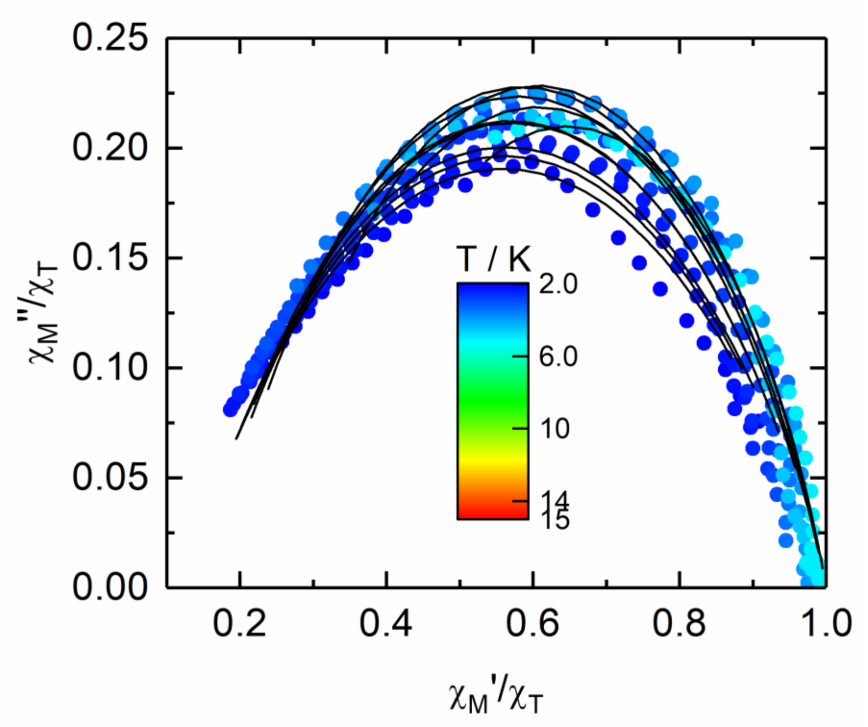

Figure S10. Normalized Argand plot for **Dy-Q** between 2 and 5 K.

Table S1. X-ray crystallographic data of **Dy-H$_2$SQ** and **Dy-Q**.

Compounds	**Dy-H$_2$SQ**	**Dy-Q**
Formula M / g.mol^{-1}	$C_{84}H_{66}Dy_2F_{18}O_{16}S_{10}$ 2318.96	$C_{86}H_{68}Cl_4Dy_2F_{18}O_{16}S_{10}$ 2486.8
Crystal system	Monoclinic	Monoclinic
Space group	C2/c (N°15)	$P2_1/c$ (N°14)
Cell parameters	a = 18.052(3) Å b = 35.748(6) Å c = 18.254(3) Å β = 92.984(7) °	a = 10.6086(11) Å b = 23.485(2) Å c = 19.414(2) Å β = 91.767(4) °
Volume / Å^3	11763(4)	4834.6(9)
Z	4	2
T / K	150 (2)	150 (2)
2θ range /°	$4.10 \leq 2\theta \leq 55.45$	$5.87 \leq 2\theta \leq 54.97$
ρ_{calc} / g.cm^{-3}	1.309	1.708
μ / mm^{-1}	1.516	1.957
Number of reflections	62737	191400
Independent reflections	13532	11074
$Fo^2 > 2\sigma(Fo)^2$	9529	9273
Number of variables	544	526
R_{int}, R_1, wR_2	0.0661, 0.0981, 0.2764	0.1219, 0.0753, 0.1607

Table S2. Best fitted parameters (χ_T, χ_S, τ and α) with the extended Debye model **Dy-Q** at 1200 Oe in the temperature range 2-5.5 K.

T / K	χ_T / cm^3 mol^{-1}	χ_S / cm^3 mol^{-1}	α	τ / s	R^2
2	9.87881	1.17843	0.47995	8.63066E-4	0.99731
2.2	9.6154	1.19238	0.46333	7.87665E-4	0.99905
2.4	9.11006	1.15028	0.45241	6.47181E-4	0.99945
2.6	8.42987	1.20621	0.41621	4.94235E-4	0.9987
2.8	8.21404	1.14112	0.41664	4.26137E-4	0.99939
3	7.56272	1.21513	0.37697	3.15642E-4	0.9989
3.5	6.71038	1.14576	0.36022	1.7472E-4	0.999
4	5.94654	1.26262	0.33113	9.66868E-5	0.99907
4.5	5.47045	1.16678	0.35391	5.23862E-5	0.99926
5	4.89902	1.44341	0.31628	3.24582E-5	0.99969
5.5	4.58454	1.27329	0.37174	1.65915E-5	0.99981

Table S3. Computed energies, *g*-tensor and wavefunction composition of the ground state doublets in the effective spin ½ model for **Dy-H$_2$SQ**.

KD	E / cm^{-1}	g_X	g_Y	g_Z	Wavefunction*
1	0	0.11	1.10	15.08	34% |±13/2> + 25% |±15/2> +15% |±11/2> + 10% |±7/2>
2	13	0.03	1.11	14.29	26% |±11/2> + 18% |±13/2> +17% |±9/2> + 11% |±7/2>
3	155	1.92	2.18	14.69	38% |±9/2> + 19% |±15/2> +17% |±11/2> + 16% |±7/2>
4	228	2.92	5.15	11.23	24% |±5/2> + 17% |±3/2> +17% |±11/2> + 13% |±1/2>
5	274	2.22	4.32	11.93	23% |±7/2> + 18% |±3/2> +18% |±1/2> + 14% |±5/2>
6	352	0.55	1.20	16.04	31% |±15/2> + 24% |±13/2> +11% |±11/2>
7	400	10.40	8.05	0.39	50% |±1/2> + 15% |±3/2> +14% |±7/2>
8	413	10.35	8.12	0.04	32% |±3/2> + 28% |±5/2> +11% |±7/2> + 11% |±9/2>

*: only components > 10% are given for sake of clarity

Table S4. Computed energies, *g*-tensor and wavefunction composition of the ground state doublet in the effective spin ½ model for **Dy-Q**.

KD	E / cm^{-1}	g_X	g_Y	g_Z	Wavefunction*
1	0	0.05	0.11	19.24	90% |±15/2>
2	80	0.14	0.26	15.86	70% |±13/2>
3	137	0.07	0.53	13.57	27% |±11/2> + 14% |±13/2> +13% |±7/2> + 12% |±5/2>
4	184	1.52	2.14	10.85	25% |±11/2> + 23% |±9/2> +19% |±5/2> + 15% |±1/2>
5	227	4.22	6.52	10.97	33% |±3/2> + 17% |±1/2> +15% |±7/2> + 13% |±5/2>
6	335	0.02	0.58	16.50	49% |±1/2> + 18% |±3/2> +11% |±9/2>
7	405	0.63	3.13	14.70	30% |±7/2> + 29% |±9/2> +12% |±3/2>
8	421	0.41	3.78	15.45	42% |±5/2> + 20% |±3/2> +18% |±7/2> + 11% |±11/2>

*: only components > 10% are given for sake of clarity